RESEARCH ARTICLE

Eleyon NANOSCALE REPORTS

DOI: 10.26524/nr1923

Structural and Electrical Properties of ZnO Varistor with Different Particle Size for Initial Oxides Materials

S.A. Amin [a, b *]

[a] Physics Department, Faculty of science, Assiut University, Assiut, Egypt.
[b] Physics Department, Faculty of Science, Taif University, Taif 888, Saudi Arabi.

***Corresponding Author**
susanamin2002@yahoo.com
(S.A. Amin)

Received : 29-02-2019
Accepted : 26-04-2019

ABSTRACT: We report here structural, electrical and dielectric properties of ZnO varistors prepared with two different particle sizes for initial starting oxides materials (5 µm and 200 nm). It is found that the particle size of ZnO does not influence the hexagonal wurtzite structure of ZnO, while the lattice parameters, crystalline diameter, grain size and Zn-O bond length are affected. The nonlinear coefficient, breakdown field and barrier height are decreased from 18.6, 1580 V/cm and 1.153 eV for ZnO micro to 410 V/cm, 7.26 and 0.692 eV for ZnO Nano. While, residual voltage and electrical conductivity of upturn region are increased from 2.08 and $2.38x10^{-5}$ $(\Omega.cm)^{-1}$ to 4.55 and $3.03x10^{-5}$ $(\Omega.cm)^{-1}$. The electrical conductivity increases by increasing temperature for both varistors, and it is higher for ZnO Nano than that of ZnO micro. The character of electrical conductivity against temperature is divided into three different regions over the temperature intervals as follows; (300 K ≤ T ≤ 420 K), (420 K ≤ T ≤ 580 K) and (580 K ≤ T ≤ 620 K), respectively. The activation energy is increased in the first region from 0.141 eV for ZnO micro to 0.183 eV for ZnO nano and it is kept nearly constant in the other two regions. On the other hand, the average conductivity deduced through dielectric measurements is increased from $2.54x10^{-7}$ $(\Omega.cm)^{-1}$ for ZnO micro to $49x10^{-7}$ $(\Omega.cm)^{-1}$. Similar behavior is obtained for the conductivities of grains and grain boundaries. The dielectric constant decreases as the frequency increases for both varistors, and it is higher for ZnO nano than that of ZnO micro. These results are discussed in terms of free excited energy and strength of link between grains of these varistors.

Keywords: A Ceramics, B Chemical synthesis, C X-ray diffraction, C Electron microscope, D Electrical properties.

1. Introduction

ZnO is an important material in various fields of applications such as varistors and gas sensors [1-5]. ZnO exhibits upturn region due to its electrostatic potential barrier formed at the grain boundaries [6-10]. The existence of the nonlinear region, in parallel with high current densities and breakdown fields, are the most significant properties of ZnO varistor. The upturn region is usually obtained at high current density beyond 10^3 A/cm^2, and breakdown fields close to 5000 V/cm. This behavior represents the voltage drop in the grains, and restricts ZnO varistors applications [1]. The behavior of nonlinear region normally depends on density, chemical composition of the compound and also nanostructure development [11-14].

However, applications of ZnO varistors for circuit Protection is highly significant due to overload electronic circuits. For instance, battery powered and mobile appliances require protection of transient dc voltage between up to 20 V, while some other devices need fast response protection up to 70 V [15, 16]. These factors create needs for continuous development of ZnO varistor with fast and higher response likes non-linear coefficient, density of localized states, dc conductivity and energy absorption capabilities at the breakdown voltage. Although, most of them have been developed towards high voltage applications of 60 nonlinear coefficient and grain boundary voltage of 3V, few attempts are directed towards low-voltage of 10 nonlinear coefficient and breakdown field of 20 V/cm, which is also required for special applications [17, 18].

The Electrical conductivity of ZnO varistor depends on the amount and nature of oxygen vacancies generated during its synthesized [19, 20]. These oxygen vacancies are controlled by several parameters such as dopants and ZnO particle size [21-24]. It has been observed that these parameters are able to increase the current density in the upturn region of ZnO varistor and also shifted its onset value to lower fields, which is therefore necessary.

It is well known that electron traps, localized at the grain boundaries of ZnO, are adsorbed oxygen and capture the electrons coming from the donor states [25]. Therefore, Schottky barrier capacitance becomes dependent on the frequency signal. This is due to the finite time constants associated with the charging and discharging of the deep trap states in the depletion layer [26, 27]. When low ac voltages ≈ 300 mV is applied across a varistor, a sinusoidal current will flow with the same angular frequency [28]. It has the great advantage over the dc techniques of being able to separate the electric response in different regions of ZnO ceramics, provided their electrical responses within the range of the instrumentation and the time constants [29, 30]. This response is characterized by the complex impedance Z as a function of the frequency. The real and imaginary parts of complex impedance with respect to the applied voltages can be determined in the frequency range up to GHz.

Nanotechnology is of growing importance in many branches of research because of the interesting properties associated with depressing the material particle size [31-33]. These nanomaterials, due to their peculiar characteristics and size effects, often show novel physical properties compared to these of bulk materials. Today, nanoparticles of metal oxides have been the focuses of a number of research efforts due to the unusual properties that are expected upon entering this nanosize regime. With this purse in mind, ZnO with two different particle sizes for starting materials (5 μm and 200 nm) are sintered in air at temperature of 1000 ^{0}C for 12 h and then quenched down to room temperature. Structural, electrical and dielectric properties are performed by using XRD and SEM techniques, dc electrical and dielectric measurements.

2. Experimental details

Two ZnO samples with different particle size (5 μm and 200 nm) are synthesized by using solid-state reaction method. The powders of ZnO are calcined at 1000 ^{0}C in air for a period of 12 hours, ground and pressed into pellets of 1cm diameter and 0.3 cm thick. The pellets are sintered in air at temperatures of 1000 ^{o}C for 12 h, and then quenched in air down to room temperature. The bulk density of the samples is measured in terms of their weight and volume. The phase purity and surface morphology of the samples are examined by using X-ray diffractmeter (XRD) using CuKα radiation and scanning electron microscope (SEM). While I-V characteristics are obtained with an electrometer (model 6517, Keithley), 5 kV dc power supply and digital multimeter. After that, the electrical resistivity (ρ = (Rℓ/A) versus temperature measurements is performed in the temperature range of (300 - 620 K). Finally, the ac impedance at room temperature is measured by using precision impedance analyzer model 4295A (40–110 MHz). The modulus of complex impedance Z and phase angle as a function of frequency (ω) are well recorded. From the impedance spectra, values of the real Z' and the imaginary Z'' parts of the complex impedance could be obtained.

3. Results and Discussions

As listed in Table 1, the bulk density of ZnO nano is higher than that of ZnO micro. The bulk densities are 82 % and 92 % of theoretical density 5.78 g/cm^3 for ZnO [34]. The crystal structure of the samples, shown in Figure 1, is hexagonal wurtzite, and no additional lines could be formed [35, 36]. The lattice parameters listed in Table 1 are calculated in terms of($c = 2d_{(002)}$, $a = 1.155d_{(100)}$).

The lattice parameters are increased from 3.20 Å, 5145 Å for ZnO micro to 3.22 Å 5.17 Å for ZnO nano, in agreement with the reported values elsewhere [37, 38]. The wurtzite structure of ZnO is usually deviates from the ideal arrangement by changing U-parameter which describing the length of bond parallel to the c- axis. U parameter listed in Table 1 is given by $U = 0.333(\frac{a}{c})^2 + 0.25$ [39]. The constant values of U-parameter (0.379) for two varistors specifies that the four tetrahedral distances stay almost constant through a distortion of tetrahedral angles due to long-range of polar interactions [40]. The Zn-O bond length (d) is calculated using the relation, $d = [(\frac{a^2}{3}) + (0.5 - U)^2 c^2]^{\frac{1}{2}}$, and listed in Table 1[41, 42]. It is clear that d increases from 2.347Å for ZnO micro to 2.361 Å for ZnO nano, which is consistent with the behavior of lattice parameter. The average crystalline

diameter D_{hkl} is determined using the following Scherer's expression [43, 44];

$$D_{hkl} = \frac{k\lambda}{\beta \cos\theta} \quad (1)$$

Where λ and β are wavelength of X-ray radiation (λ = 1.5418 Å) and half maximum line width, respectively, θ is Bragg angle and K = 0.93 is constant. D_{hkl} value, given in Table 1, is decreased from 63.96 nm for ZnO mico to 31.15 nm for ZnO nano.

The surface morphology shown in Figure 2 indicates that the surface is rough and contains grains of crystallites which nearly having very varied shapes of different sizes. Furthermore, the crystallites are randomly distributed and irregularly disoriented, and there is no additional phases created at the boundaries of grains. In ZnO micro, the size and shape of grains are little bit different and there is a granular precipitation on the mother grains in the matrix structure. While, the grains appear with relatively small size and interfered with each other for ZnO Nano. The average grain size (D) is determined by the expression, $D = \frac{1.56L}{MN}$,

Where L is the random line length on the micrograph, M is the magnification of the micrograph, and N is the number of the grain boundaries intercepted by the lines [45]. The average grain sizes listed in Table 1 are 2.21 and 1.57 µm for ZnO micro and ZnO Nano. However, the average crystalline diameters obtained from XRD are smaller than that of SEM. This because XRD analysis determines the average diameter of crystallite's which have the same orientation inside the grain, while SEM determines the average size of grain itself. It is well known that each grain may be contains lot of crystallites with the same orientations.

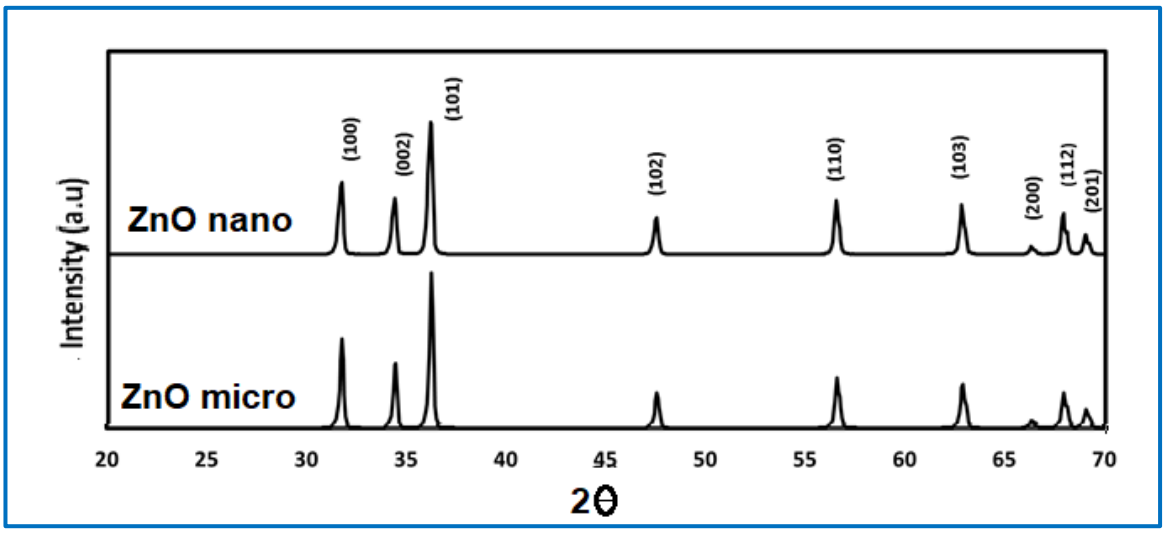

Figure 1: XRD of ZnO micro and ZnO nano varistors

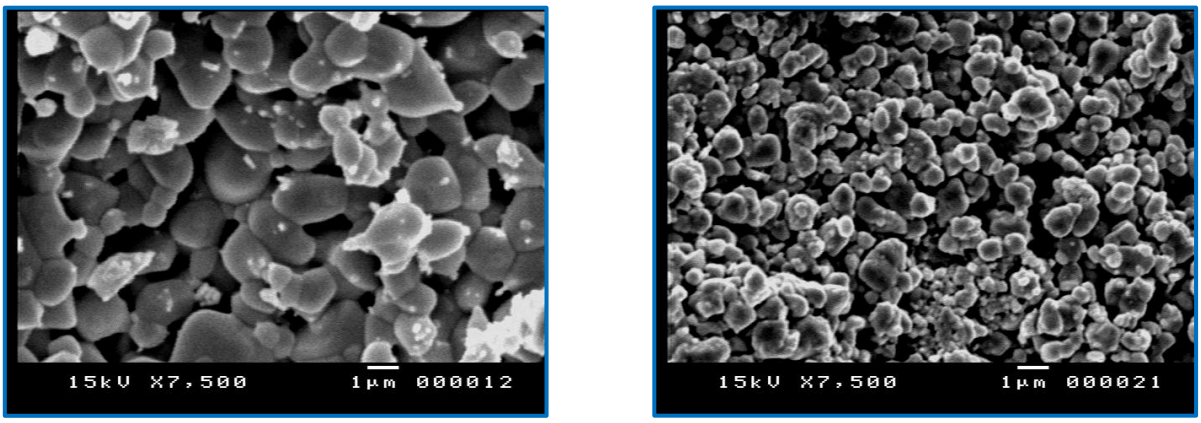

ZnO micro **ZnO nano**

Figure 2: SEM images of ZnO micro and ZnO nano varistors

Table 1: Density, lattice parameters, U-parameter, grain size , breakdown field, nonlinear coefficient , electrical conductivity, residual voltage and activation energy for ZnO micro and ZnO nano samples

Parameter	ZnO micro	ZnO nano
ρ (gm/cm^3)	4.76	5.31
a(Å)	3.203	3.224
c(Å)	5.145	5.171
U-parameter	0.379	0.379
L (Å)	2.347	2.361
D_{khl} (nm) [XRD]	63.96	31.15
Grain size(μm) [SEM]	2.21	1.57
E_B(V/cm)	1580	410
α_2	18.6	7.26
Φ_B(eV)	1.153	0.692
σ_1 (Ω.cm)$^{-1}$	2.20x10^{-7}	2.47x10^{-6}
σ_2 (Ω.cm)$^{-1}$	2.38x10^{-5}	3.03x10^{-5}
K_r	2.08	4.55
E_a(eV) (300-420 K)	0.141	0.183
E_a(eV) (420-580 K)	0.351	0.346
E_a(eV) (580-620 K)	0.831	0.842
Average cond.(Ω.cm)$^{-1}$	2.54x10^{-7}	49x10^{-7}
Grain cond. (Ω.cm)$^{-1}$	5.17x10^{-3}	11.77x10^{-3}
Grain boundary cond. (Ω.cm)$^{-1}$	1.08x10^{-6}	3.17x10^{-6}

It is evident from I-V curves shown in Figure 3 that there are three different regions observed in both varistors. The first and third regions are nearly ohmic behavior, while the second region is nonlinear (upturn region). It is also noted that the nonlinear region is weaker for ZnO nano than that of ZnO micro, but it is not completely deformed. While, the current is shifted to higher values for ZnO nano as compared to ZnO. The breakdown field E_B is usually taken as the field applied when the current flowing through the varistor is 1 mA/cm^2 [44,45]. The values of E_B listed in Table 1 are 1580 V/cm and 410 V/cm for ZnO micro and ZnO nano, respectively. This means that E_B of ZnO micro is approximately 3.85 times of E_B for ZnO nano.

The current - voltage relation of a varistor is given by the following equation [46, 47];

$$J = (\frac{E}{C})^{\alpha} \qquad (2)$$

Where J is the current density, E is the applied electric field, C is a proportionality constant corresponding to the resistance of ohmic resistor (nonlinear resistance), α is the nonlinear coefficient (α = logV/logI).

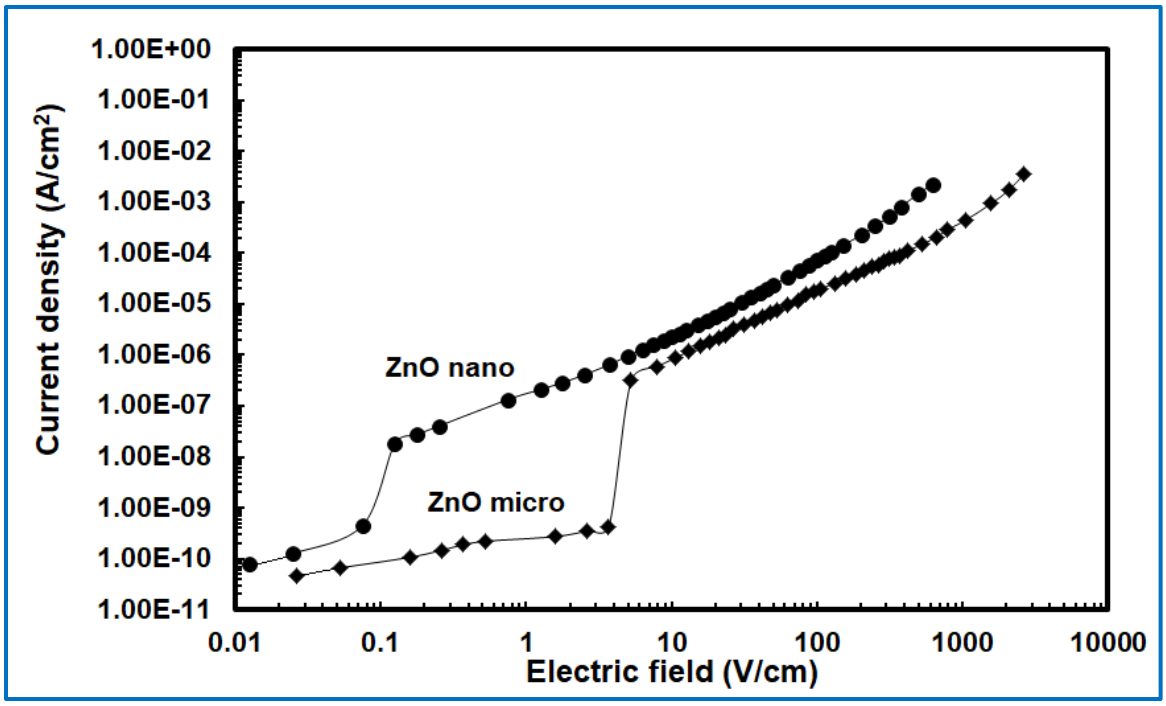

Figure 3: I-V Characteristics for ZnO micro and ZnO nano varistors

To obtain the value of α, the current - voltage curves are plotted on a log-log scale, from which the slope of the curve gives the value of α. It is apparent that α_2 for the second region is decreased from 18.6 for ZnO micro to 7.26 for ZnO nano ($\alpha_{ZnOmico}$ = 2.56 $\alpha_{ZnOnano}$). From these results, it is determined that nano material depressed the non-ohmic features of ZnO and shifts the breakdown fields to lower values. The empirical formula for the relation between K_r and E_B for a varistor is given by [48];

$$K_r = b_0 + \frac{b_1}{E_B} \qquad (3)$$

b_0 and b_1 are 1.21 and 1370 V/cm. Since the thickness of ZnO micro and ZnO nano is similar, we have calculated K_r in terms of the values of E_B given in Table 1. The values of K_r are found to be 2.08 and 4.55 V/cm for ZnO micro and ZnO nano. This of course is in good agreement with the previous studies indicating that low residual voltage ratio provides high nonlinearity coefficient and breakdown field, while the high residual voltage ratio indicates low nonlinearity coefficient and breakdown field [49].

The electrical conductivity σ_1 at room temperature is calculated in the first ohmic region by using the ohmic relation, $J = \sigma_1 E$ [50]. It is clear form Table 1 that σ_1 is 2.47×10^{-6} $\Omega^{-1}.cm^{-1}$ for ZnO nano, which is about 10 times higher than that of ZnO micro (2.20×10^{-7} $\Omega^{-1}.cm^{-1}$). For more evidence for decreasing the values of α and E_B in the present case, we have calculated the electrical conductivity σ_2 in the upturn region using the following formula [51];

$$\sigma_2 = \sigma_1 \exp\{\frac{(\alpha-1)(E_2-E_1)}{E_2}\} \qquad (4)$$

E_1 and E_2 are the applied fields across the boundaries of nonlinear region. The values of E_1, E_2, σ_1 and σ_2 across the two regions are listed in Table 1. It is observed that the values of σ_2 are 2.38×10^{-5} $\Omega^{-1}.cm^{-1}$ and 3.03×10^{-5} $\Omega^{-1}.cm^{-1}$ for ZnO micro and ZnO nano, which indicates that σ_2 for ZnO nano is approximately 1.3 times higher than that of ZnO micro.

According to Schottky type grain boundary barriers, the current density in the ohmic region of the varistor is related to the electric field by the following formula [52, 53];

$$J = AT^2 \exp\frac{BE^{\frac{1}{2}} - \phi_B}{K_B} \qquad (5)$$

where A is the Richardson's constant {A = $(4\rho emK^2 / h^3)$}, ρ is the varistor density, e is the electronic charge, m is the electronic mass, k is the Boltzmann constant, h is the Planks constant, φ_B is the interface barrier height and B is a constant. By measuring the current density in the ohm ic region and keeping the temperature constant, for two different values of applied

fields, the values of φ_B can be easily obtained. It is found that φ_B is decreased from 1.153 eV for ZnO micro to 0.692 eV for ZnO nano, in consistent with the above behaviors for E_B, α and σ.

The electrical resistivity shown Figure 4 (a) is decreased by increasing temperature for both varsitors, but it is higher for ZnO micro than that of ZnO nano. From the values of resistivity, the electrical conductivities versus temperature could be obtained, and shown in Figure 4 (b). However, the conductivity-temperature dependence is found to obey the well-known Arrhenius relation [54];

$$\sigma = \sigma_0 \exp .(\frac{-E_a}{K_B T}) \quad (6)$$

Where σ and σ_o are the electrical conductivities at temperatures T and T_o (0K), and E_a is the activation energy. Within the temperature range selected for the conductivity measurements, it is possible to distinguish discrete regions corresponding to different activation energies. The character is divided into three regions over the temperature intervals as follows; (300 K ≤ T ≤ 420 K), (420 K ≤ T ≤ 580 K) and (580 K ≤ T ≤ 620 K), respectively.

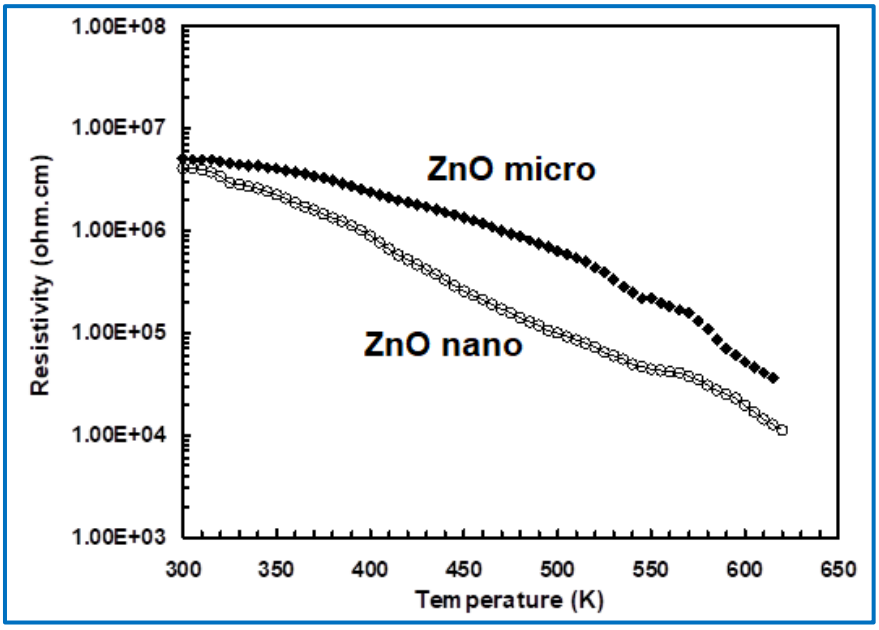

Figure 4(a): Resistivity versus temperature for ZnO micro and ZnO nano varistors

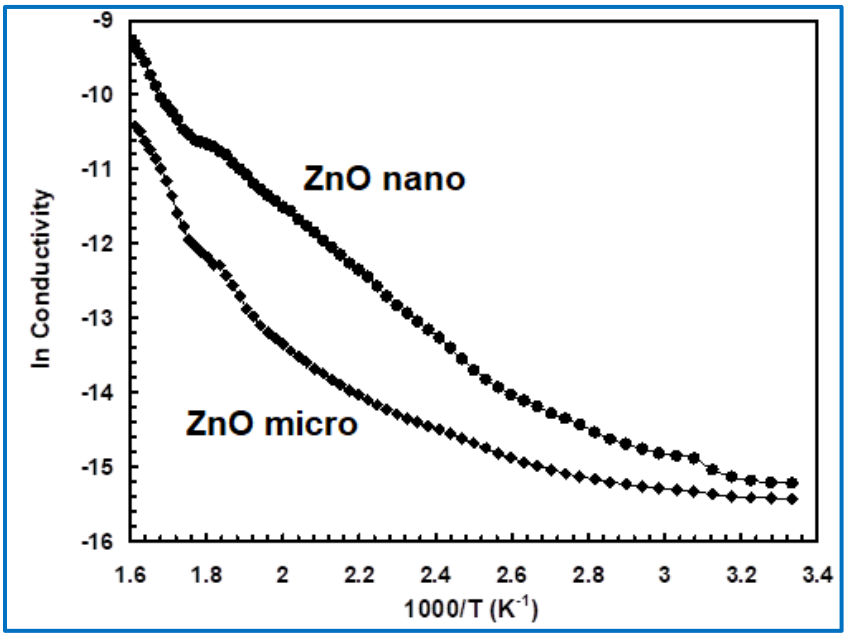

Figure 4(b): Conductivity versus temperature for ZnO micro and ZnO nano varistors

The values of the activation energy E_a are calculated from the slope of each plot by using the above logarithmic relation and listed in Table 1.

The values of E_a are 0.141 eV, 0.351 eV and 0.831 eV for ZnO, 0.183 eV, 0.346 eV and 0.842 eV for ZnO nano. The activation energy is increased in the first region from 0.141 eV for ZnO micro to 0.183 eV for ZnO nano and it is kept nearly constant in the other two regions. These values indicate that the band energy gap is increased as the temperature increases, and it is approximately the same for both variators in the second and third regions, in consistent with the previous investigations based on ZnO varistor [55, 56].

In case of Cole-Cole model, the impedance representation is expressed by the following empirical relation [57, 58]:

$$Z(\omega) = Z_{\infty}^{*} + \frac{Z_{0\infty}^{*}}{1+(j\omega\tau_{p})^{1-\gamma}} \qquad (7)$$

Where $Z_{0\infty}{}^{*}$ is the impedance at infinite frequency, $Z_{0\infty}{}^{*} = Z_{0}{}^{*} - Z_{\infty}{}^{*}$, $Z_{0}{}^{*} = Z_{0}{}^{*}(w), as\ \omega \to 0,$ where ω = 2πf and τ_o can be calculated from $\omega\tau_o = 1$ at the summit of the semicircle. $\gamma = (2\theta/\pi)$ and $(1 > \gamma > 0)$, and τ_p is the relaxation time calculated from $\omega\tau_p = 1$ at the summit of the arc [59]. Figure 4 shows the real part of ac impedance versus imaginary part at different frequencies. It is clear that ZnO micro shows one semicircle, while one quarter of a circle is shown for ZnO nano. From these curves, the average grain and grain boundary conductivities are calculated and summarized in Table 1. As evidenced in Table 1, the conductivity of grains for ZnO nano is about 10^3 times more than the conductivity of the grain boundaries. Moreover, the conductivity of ZnO nano is always higher than that of ZnO micro. However, it has been found that the impedance spectra of calcined ZnO micro exhibited two arcs. The first arc at a low frequency is interpreted due to the grain boundary effect while the second arc at a high frequency region is attributed to the grain's effects [60, 61]. While, a single arc is observed in all spectra of sintered ZnO micro [62, 63] as we obtained. The single arc means that the conduction processes through the grain and grain boundary has identical time constants, $\tau = (1/\omega) = RC$. This behavior indicates that the conduction in the grain and grain boundary occurs in the same process and could not be separated by the impedance spectroscopy [64, 65]. The dielectric constant as a function of frequency (lnf) for the varistors is represented in Figure 5. It is apparent that the dielectric constant is decreases as the frequency increases for both varistors, but it is higher for ZnO nano as compared to ZnO micro, in agreement with the behavior of conductivity. Based on the above results, we can gather conclude that the probability of nano particles rush into the grain boundaries is very high at the considered sintering temperature.

According to previous reports, three different values for optical band gap (3.1, 3.2 and 3.3 eV) and (40-60 mV) free excited energy have been reported ZnO at room temperature [66, 67]. For band-gap energy E_g determination, it was assumed that the fundamental absorption edge of ZnO-X metal oxide is due to the direct allowed transition.

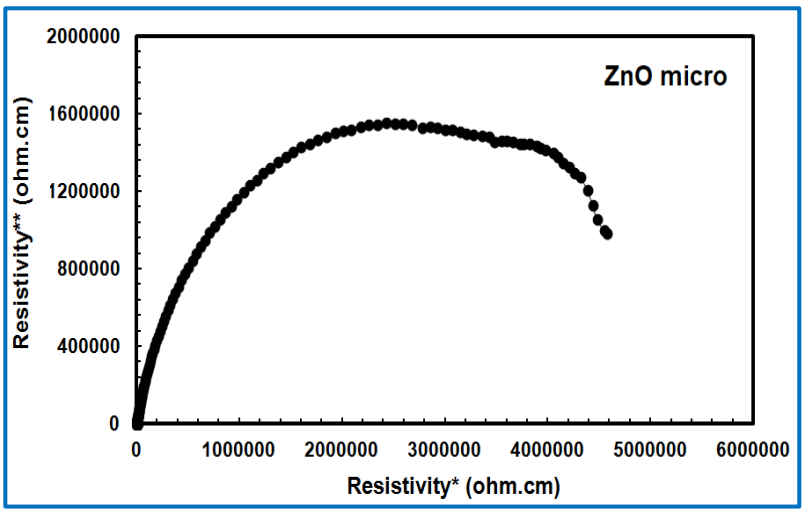

Figure 5(a): Z^{**}versus Z^{*} for ZnO micro varistor

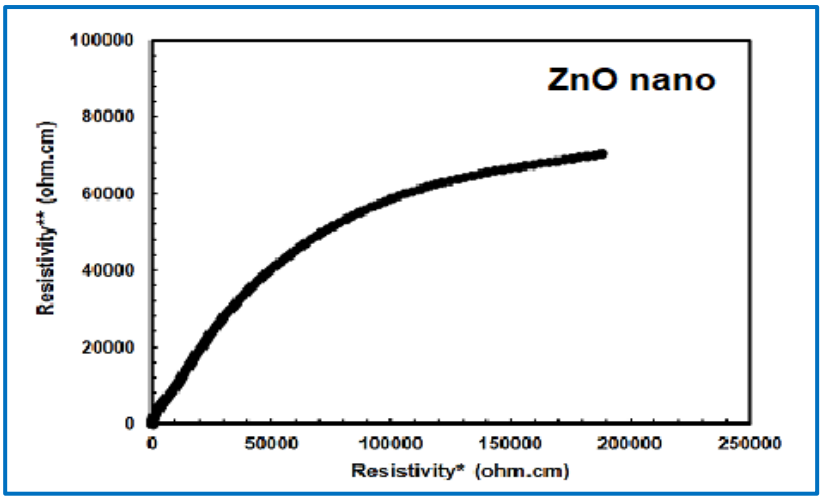

Figure 5(b): Z^{**} versus Z^{*} for ZnO nano varistor

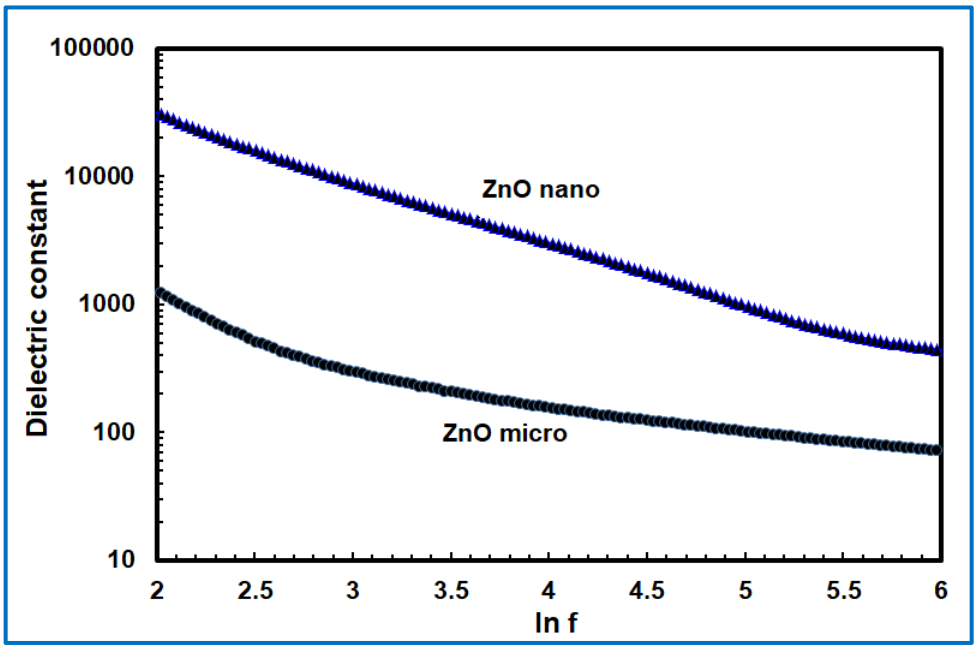

Figure 6: Dielectric constant versus lnf for ZnO micro and ZnO nano varistors

So, we believe that although E_g is nearly the same for both varistors, the free excited energy may be less in ZnO nano as compared to ZnO micro. Decreasing the free excited energy helps for improving the electrical conductivity of ZnO nano, and consequently the potential barrier is weakness. Furthermore, the small size of grains of ZnO nano , as compared to ZnO, micro are able to localize together at the grain boundaries, and helps for producing some other sensitive intergrain conduction paths. These conduction paths can operate in parallel through the grain boundary region and weakness the potential barriers of ZnO varistors, in agreement with the present data. This is of course is supported by a good correlation between behaviors of grain size, nonlinear coefficient, breakdown field, electrical conductivity and dielectric constant.

4. Conclusion

Structural and electrical properties of ZnO varistor with two different particle sizes for initial oxides materials are performed. We have shown that the particle size does not influence the wurtzite structure of ZnO, while the lattice parameters, crystalline diameter, grain size and Zn-O bond length are affected. The potential barrier of 18.6 nonlinear coefficients could be formed for ZnO microsize, but it is decreased 7.26 for ZnO nanosize. Furthermore, the ZnO nanosize decreased the breakdown

field from 1580 V/cm to 410 V/cm, increased residual voltage from 2.08 to 4.55 and decreased the electrical conductivity of upturn region from $2.38x10^{-5}$ $(\Omega.cm)^{-1}$ to $4.97x10^{-7}(\Omega.cm)^{-1}$. Moreover, the activation energy in the first region increased from 0.128 eV for ZnO microscale to 0.164 eV for ZnO nanoscale, but it is completely unaffected in the other two regions. Finally, the dielectric constant could be improved by decreasing the ZnO particle size. It is believed that the free excited energy and the strength of link between ZnO grains are responsible for the present behavior.

References

[1] L.M. Levinson, H. R. Phillip, *American Ceramics Society Bulletin*, 65 (1986) 639.

[2] T.K. Gupta, Application of Zinc Oxide Varistors, *Journal of American Ceramic Society*, 37 (1990) 1817.

[3] N.W. Emanetoglu, C Gorla, Y Liu, S Liang, Y Lu, Epitaxial ZnO piezoelectric thin films for saw filters, *Materials Science in Semiconductor Processing*, 2 (1999) 247-252.

[4] R. Paneva, D. Gotchev, Non-linear vibration behavior of thin multilayer diaphragms, *Sensors Actuators A: Physical*, 72 (1999) 79-87.

[5] Lian Gao, Qiang Li , Weiling Luan, Hirokazu Kawaoka, Tohru Sekino, Koichi Niihara, Preparation and Electric Properties of Dense Nanocrystalline Zinc Oxide Ceramics, *Journal of American Ceramic Society*, 85 (2002) 1016-1018.

[6] M. Matsouka, Nonohmic Properties of Zinc Oxide Ceramics, *Nonohmic Properties of Zinc Oxide Ceramics*, 10 (1971) 736-746.

[7] K. Mukae, K. Tsuda, I. Nagasawa, Capacitance - vs - voltage characteristics of ZnO varistors, *Journal of Applied Physics*, 16 (1977)1361.

[8] G.E. Pike, C.H. Seager, The dc voltage dependence of semiconductor grain - boundary resistance, *Journal of Applied Physics*, 50 (1979) 3414.

[9] Fumiyasu Obe, Yukio Sato, Takahisa Yamamoto, Yuichi Ikuhara, Taketo Sakuma, Current-Voltage Characteristics of Cobalt - Doped Inversion Boundaries in Zinc Oxide Bicrystals, *Journal of American Ceramic Society*, 86 (2003) 1616-1618.

[10] Zhen Zhou, K. Kato, T. Komaki, M. Yoshino, H.Yukawa, M.Morinaga and K.Morita , Effects of dopants and hydrogen on the electrical conductivity of ZnO, Journal of the European Ceramic Society, 24 (2004)139-146.

[11] T.K. Gupta, Microstructural engineering through donor and acceptor doping in the grain and grain boundary of a polycrystalline semiconducting ceramic, *Journal of Materials Research,* 7 (1992) 3280-3295.

[12] M. Inada, J pn .J. appl. Phys. 19 (1980) 409.

[13] E. Olsson, G.L. Dunlop, R. österlund, Development of Functional Microstructure during Sintering of a ZnO Varistor Material, *Journal of American Ceramic Society*, 76 (1993) 61.

[14] Choon - Woo Nahm and Byoung – Chil Shin, *Materials Letters*, 57 (2003)1322-1326.

[15] W.H. Pan, S.T. Kuo, W.H. Tuan, H.R. Chen, Microstructure–Property Relationships for Low-Voltage Varistors, *International Journal of Applied Ceramic Technology*, 7 (2010) E80-E88.

[16] Wan Rafizah Wan Abdullah, Azmi Zakaria and MohdSabriMohdGhazali, Synthesis Mechanism of Low-Voltage Praseodymium Oxide Doped Zinc Oxide Varistor Ceramics Prepared Through Modified Citrate Gel Coating, *International Journal of Molecular Sciences,* 13 (2012) 5278-5289.

[17] C.W. Nahm, The preparation of a ZnO varistor doped with and its properties, *Solid State Communications*. 149 (2009) 795–798.

[18] N. Horio, M. Hiramatsu, M. Nawata, K. Imaeda, T. Torii, Preparation of zinc oxide/metal oxide multilayered thin films for low-voltage varistors, *Vacuum*, 51 (1998) 719-722.

[19] J.M. Madou and R. S. Morrison, (1989) Chemical Sensing with Solid State Devices, *Academic Press*, San Diego, CA.

[20] P. Bonasewicz, W. hirscawald, G. Newnann, The investigation of the pressure and temperature dependence of the electrical conductivity of thin zinc oxide films with high resistances, *Physica Status Solidi (a) banner*, 97 (1986) 593.

[21] G. W. Clarson, K.T. Gupta, Improved varistor nonlinearity via donor impurity doping, *Journal of Applied Physics*, 53(1982) 5746.

[22] L.Y. Tsai, L.C. Huang, C.C. Wei, Improvement of nonlinearity in a ZnO varistor by Al2O3 doping, Journal *of Materials Science Letters,* 4 (1985) 1305-1307.

[23] Jiaping Han, P.Q. Mantas, A.M.R. Senos, Effect of Al and Mn doping on the electrical conductivity of ZnO, *Journal of the European Ceramic Society*, 21(2001) 1883-1886.

[24] J. Han, Q.P. Mantas, A.M.R. Senos, P.Q. Mantas, Densification and Grain Growth of AI-Doped Zno, *Journal of Materials Research*, 16 (2001) 459 -468.

[25] L. C. Sleston, M. E. Potter, A. M. Alim, *Journal of American Ceramic Society*, 71 (1987) 909.

[26] R. Eizinger, Surf. Sci, 1 (1978) 329.

[27] S. ezhilvalavan and T. R. N. Kutty, High‐frequency capacitance resonance of ZnO‐based varistor ceramics, *Applied Physics Letters*, 69 (1996) 3540.

[28] Agnes Smith, Jean Francois baumard, Pierre Abelard, ac impedance measurements and V-I characteristics for Co-, Mn-, or Bi-doped ZnO, *Journal of Applied Physics*, 65 (1989) 5119.

[29] M. Andres Verges and A. R. West, Impedance and Modulus Spectroscopy of ZnO Varistors, *Journal of Electroceramics*, 1 (1997) 125-132.

[30] M. Peiteado, M.A. de la Rubia, M.J. Velasco, F.J. Valle, A.C. Caballero, Bi2O3 vaporization from ZnO-based varistors, *Journal of the European Ceramic Society*,25 (2005) 1675-1680.

[31] L.D. Marks, Reports on Progress in Physics Experimental studies of small particle structures, *Reports on Progress in Physics,* 57 (1994) 603.

[32] M.L. Dinesha , H.S. Jayanna , S. Ashoka , G.T. Chandrappa, Temperature dependent electrical conductivity of Fe doped ZnO nanoparticles prepared by solution combustion method, *Journal of Alloys and Compounds*, 485 (2009) 538-541.

[33] M.S. Castro, C.M. Aldao, Effects of the Sintering Temperature on the Oxygen Adsorption in ZnO Ceramics, *Journal of the European Ceramic Society*, 19 (1998) 511-515.

[34] G. Pei, C. Xia, S. Cao, J. Zhang, F. Wu, J. Xu, *Journal of Magnetism and Magnetic Materials*, 302 (2006) 340.

[35] Bates, H. Carl, White, B. William, Roy, Rustum, New High-Pressure Polymorph of Zinc Oxide, *Science*, 137 (1962) 993.

[36] Guangqing Pei, Changtai Xia, Shixun Cao, Jungang Zhang, Feng Wu, Jun Xu, Synthesis and magnetic properties of Ni-doped zinc oxide powders, *Journal of Magnetism and Magnetic Materials*, 302 (2006) 340-342.

[37] A.Sedky, Ayman sawalha and Amal Yaseen, Enhancement of Electrical Conductivity by Al doped ZnO Ceramic Varistors, *Physica B*, 404 (2009) 3519.

[38] E. Kisi, M.M. Elcombe, u parameters for the wurtzite structure of ZnS and ZnO using powder neutron diffraction, *Acta Crystallographic, Section C*, 45 (1989) 1867-1870.

[39] Ü. Özgür, A. Ya, I. Alivov, C. Liu, A. Teke, M. A. Reshchikov, S. Doğan, V. Avrutin, S. J. Cho, H. Morkoçd, A comprehensive review of ZnO materials and devices, *Journal of Applied Physics*, 98 (2005)1301.

[40] A. Sedky, S. B. Mohamed, Effect of temperature on the electrical properties of $Zn_{0.95}M_{0.05}O$ (M = Zn, Fe, Ni), *Materials Science-Poland*, 32 (2014) 16-22.

[41] S. Aksoy, Y. Caglar, S. Ilican, M. Caglar, Effect of deposition temperature on the crystalline structure and surface morphology of ZnO films deposited on p-Si, *Advances in Control, Chemical Engineering, Civil Engineering and Mechanical Engineering*, (2010) 227-231.

[42] U. Seetawan, S. Jugsujinda, T. Seetawan, A. Ratchasin, C. Euvananont, C. Junin, C. Thanachayanont, P. Chainaronk, Effect of Calcinations Temperature on Crystallography and Nanoparticles in ZnO Disk, *Materials Sciences and Applications*, 2 (2011) 1302-1306.

[43] B.D. Cullity, S.R. Stock, (2001) Elements of X-ray Diffraction, 3rd Edition, *Prentice Hall*, Upper Saddle River.

[44] J. C. Wurst, J. A. Nelson, Lineal Intercept Technique for Measuring Grain Size in Two‐Phase Polycrystalline Ceramics, *Journal of American Ceramic Society*, 55 (1972) 109.

[45] V.V. Deshpande, M.M. Patil, V. Ravi, Low voltage varistors based on CeO2, Ceramic international, 32 (2006) 85-87.

[46] V.V. Deshpande, M.M. Patil, V. Ravi, Low voltage varistors based on CeO2, Ceramic international, 32 (2006) 85-87.

[47] M. Matsuoka, Nonohmic Properties of Zinc Oxide Ceramics, *Japanese Journal of Applied Physics*, 10 (1971) 736-746.

[48] Shengtao Li, Feng Xie, Fuyi Liu, Jianying Li, Mohammad A. Alim, The Relation Between Residual Voltage Ratio and Microstructural Parameters of ZnO Varistors, *Materials Letters*, 59 (2005) 302-307.

[49] J. Han, P.Q. Mantas and A.M.R. Senos, Effect of Al and Mn doping on the electrical conductivity of ZnO, *Journal of the European Ceramic Society*, 21 (2001)1883-1886.

[50] A.Sedky, M. Abu-Abdeen and Abdul-Aziz A. Almulhem, Nonlinear I–V characteristics in doped ZnO based-ceramic varistor, *Physica B Condensed Matter B*, 388, (2007) 266-273.

[51] A. Sedky, A suitable Model for Nonlinear Conduction Region in ZnO Ceramic Varistors, *International J of Photonics and Optical Technology* 3 (2017) 1-3.

[52] S.R. Dhage, Vandana Choube, V. Ravi, Nonlinear I–V characteristics of doped SnO2, *Material Science Engineering B,* 110 (2004) 168-171.

[53] E.E. Hahn, Some Electrical Properties of Zinc Oxide Semiconductor, *Journal of Applied Physics*, 22 (1951) 855.

[54] G. Heiland, E.Mollowo, F. Stockmann, Electronic Processes in Zinc Oxide, *Solid State Physics*, 8 (1959) 191-323.

[55] B.Z.Azmi, Zahid Rizwan, M. Hashim, A.H. Shaari, W.M.M. Yunus and E. Saion, *American Journal of Applied Sciences*, 22 (2005).

[56] V. Srikant, D.R. Clarke, on the optical band gap of zinc oxide, *Journal of Applied Physics*, 83(1998) 5447.

[57] K. H. Cole and R. H. Cole, Dispersion and Absorption in Dielectrics I. Alternating Current Characteristics, *The Journal of Chemical Physics*, 9 (1941) 341.

[58] K. Al Abdullah, A. Bui and A. Loubiere, Low frequency and low temperature behavior of ZnO‐based varistor by ac impedance measurements, *Journal of Applied Physics*, 69 (1991) 4046.

[59] R. Bartnikas, R. M. Eichhorn, (1983) eds. Engineering Dielectrics, (ASTM) Philadelphia IIA, 69.

[60] Y. Dutuit, La transformation de Fourier discrète en spectroscopie temporelle, *Journal of Applied Physics*, 14 (1979) 939-945.

[61] J. Jose, Abdul Khadar, Role of grain boundaries on the electrical conductivity of nanophase zinc oxide, *Materials Science and Engineering: A*, 304 (2001) 810-813.

[62] J. Jose, Abdul Khadar, Impedance spectroscopic analysis of AC response of nanophase ZnO and ZnO-Al2O3 nanocomposites, *Nanostructured Materials*, 11 (1999) 1091-1099.

[63] J. Jose, Abdul Khadar, Role of grain boundaries on the electrical properties of ZnO–Ag nanocomposites: an impedance spectroscopic study, *Acta Materialia*, 49 (2001) 729-735.

[64] W. C. Nan, Grain size-dependent electrical properties of nanocrystalline ZnO, *Journal of Applied Physics*, 85 (1999) 7735.

[65] Z. Brankoviz, G. Brankoviz, D. Poleti, A. J. Varela, Structural and electrical properties of ZnO varistors containing different spinel phases, *Ceramics international*, 271 (2001) 115-122.

[66] Z. Brankoviz, G. Brankoviz, D. Poleti, A. J. Varela, Structural and electrical properties of ZnO varistors containing different spinel phases, *Ceramics international*, 271 (2001) 115-122.

[67] Zhen Zhou, K. Kato, T. Komaki, M. Yoshino, H. Yukawa, M. Morinaga, K. Morita, Effects of dopants and hydrogen on the electrical conductivity of ZnO, *Journal of the European Ceramic Society*, 24 (2004) 139-146

Acknowledgements

The authors would like to thank Prof. Dr/ A.Sedky, Assiut University and Prof. Dr/ Atif Mossad, Physics Department, King Khalid University, Saudi Arabia University for co-operation during the present investigation.

Competing Interests: The author declares to have no competing interests

About The License